REVIEWS OF MODERN PHYSICS VOLUME 45, NUMBER 1 JANUARY 1973

Quasi-Free Scattering and Nuclear Structure. II.

GERHARD JACOB* AND TH. A. J. MARIS

Instituto de Física, Universidade Federal do Rio Grande do Sul,† Pôrto Alegre, RS, Brasil

This complement of an earlier paper [Rev. Mod. Phys. **38**, 121 (1966)] reviews experimental and theoretical progress made since 1965 in the knowledge of quasi-free $(p, 2p)$ and $(e, e'p)$ processes in nuclei. Some aspects of the reaction mechanism are considered and a new method to present the experimental data is suggested. The character of the final hole states is discussed. New experimental results are presented and the available information on "hole-spectroscopy" is summarized. Several open problems are pointed out.

CONTENTS

1. INTRODUCTION

Quasi-free scattering processes have, during the last fifteen years, proven a useful tool for the investigation of the nuclear shell model; in particular so far as strongly bound shells are concerned, these reactions are at present nearly unique.

The considerable amount of experimental and theoretical work which has been performed since the writing of our earlier review (JM66) (hereafter to be referred to as I), has rendered that paper incomplete, though its content does not seem to need a revision. For this reason the present paper should be considered as an updating of I, which is assumed to be known.

Several instructive reviews on $(p, 2p)$ reactions (BT66, Jac68, Wi68, Be69, Ku69, RR69, Ja71) and $(e, e'p)$ processes (CS66, Am67, Fo67, Am70, At71, Üb71) have appeared in recent years. Our work differs somewhat from these papers in that we discuss the theory and experiments of both reactions from a unified point of view, which we try to keep as physical as possible.

As in our earlier paper we shall limit ourselves essentially to quasi-free proton–proton and electron–proton scattering [i.e., to $(p, 2p)$ and $(e, e'p)$ reactions] in nuclei with $A \geq 4$, and to incident energies higher than 150 MeV for incoming protons and higher than 300 MeV for incoming electrons. We think that the descriptions and the theoretical approximations in the two mentioned cases should be essentially different from the ones of, e.g., quasi-free proton–deuteron and proton–alpha scattering. The reason for this is that at the considered energies the proton is an elementary particle, whose structure inside the nucleus is only slightly influenced by the neighboring nucleons; therefore one can consider, under suitable circumstances, its scattering as being quasi-free. A similar situation will in general be only poorly approximated in the case of the deuteron and the alpha particle which doubtlessly are to a good part "dissolved" in the nucleus in most cases (WC66).

The quasi-free reactions have two main aspects which are relatively independent:

(a) the reaction mechanism; i.e., the properties and limitations of the impulse approximation, and the initial and final state interactions; and

(b) the properties of the states of the residual nuclear system.

Aspect (a) differs sharply for $(p, 2p)$ and $(e, e'p)$ scattering, but, with respect to aspect (b), these processes overlap strongly. Although the separation into (a) and (b) is of course not a complete one, we shall nevertheless divide most of our discussion in that way. This is particularly convenient because nearly all theoretical papers have concentrated, according to the interest of the authors concerned, on only one of the two aspects, treating the other one very summarily.

In the next Section we shall discuss some new theoretical developments and Section 3 presents recent experimental results. Some open problems are discussed in Section 4.

The subject under consideration is related to several areas of nuclear physics. Therefore, we have not attempted to give a complete list of References, but have limited ourselves to mentioning only the work directly connected to our discussion.

2. THEORETICAL DEVELOPMENTS

Although most of the progress in the last five years has been in the experimental aspects of quasi-free scattering, strikingly confirming the general viewpoint taken in I, some interesting theoretical developments have also taken place. We shall first discuss some points which are directly related to the reaction mechanism, and then the ones which are more concerned with the

* Senior Research Fellow, Conselho Nacional de Pesquisas.
† Work supported by U.S. Army Research Office, Banco Nacional do Desenvolvimento Econômico, Conselho Nacional de Pesquisas, Conselho de Pesquisas UFRGS, and Regional Program of Scientific and Technological Development of the OAS.

understanding of the nuclear states resulting from a quasi-free scattering process.

2.1 Reaction Mechanism

As was seen in I, the problem of distortion is essential for $(p, 2p)$ experiments (where absorptions of more than 90% due to multiple collisions are no exception), but is only of minor importance for $(e, e'p)$ processes (where over-all reduction factors between 0.5 and 0.8 are the rule). As earlier, we are considering those cases where the energy of each of the outgoing protons is at least approximately 70 MeV; for the strong effect of distortion at energies below this limit we refer, e.g., to (CT69) for $(p, 2p)$ reactions, and to (VA71) for $(e, e'p)$ reactions.

The angular correlation of the two outgoing protons in a quasi-free $(p, 2p)$ experiment is given by

$$d\sigma/dE_1d\Omega_1dE_2d\Omega_2=[4/(\hbar c)^2]$$
$$\times(k_1k_2\bar{E}_0^2/k_0E_3)(d\sigma^{fr}/d\bar{\Omega})(2J_A+1)^{-1}$$
$$\times\sum_{m_{A-1},m_A}\sum_n|g'^{(n)}{}_{m_{A-1},m_A}(\mathbf{k}_1+\mathbf{k}_2-\mathbf{k}_0)|^2$$
$$\times\delta(E_1+E_2+E_{A-1}-E_0-E_A). \quad (\text{I3.31})$$

Up to now, the approximate evaluation of this expression has only given semiquantitative agreement with experiment (PB72). This is true both for the shape and for the absolute magnitude of the angular distribution (deviations by factors of order 1 are common). One of the reasons for the disagreement is the approximate treatment of the distortion which we therefore discuss in some more detail.

In determining the distortion of the incoming and outgoing proton waves, the first question which arises concerns the choice of the size and shape of the distorting complex optical potential, which in all calculations up to now has been taken spin independent.

The most direct way to choose this potential would be to take it from an analysis of elastic scattering at the appropriate energies. This, however, may not be the best way because the elastic and quasi-free scattering results are sensitively dependent on rather different properties of the optical potential; a potential which is very good for one of the processes may be rather bad for the other.

Therefore, at the energies considered, it is probably better to derive the optical potential directly from the nucleon–nucleon cross section (Wa53, FW53, KMT59), taking the local nuclear density and the Pauli principle into account (Go48, LMT59, DS63). The potential thus calculated should of course still be in reasonable agreement with that found from elastic scattering experiments. However, one is in this way able to improve the distorting potential for quasi-free processes in certain points which have almost always been neglected.

Because of the large total path of the incoming and outgoing nucleons in the nucleus, a good part of the contribution to the quasi-free cross section comes from the region of the nuclear surface where the distorting potential is small and the wave function of the particle to be ejected is not yet negligible. Therefore the cross section is strongly dependent on the overlap between the nucleon wave function and the distorting potential in this region. In most calculations a shape for the optical potential (square well, Gaussian, Woods–Saxon, etc.) has been used which is rather unrelated to the nuclear density distribution. One exception is in (HJMS71), where the effect of changes in this shape for a fixed nuclear density was investigated. As expected, the results show clearly that the calculated angular correlation is sensitively dependent, both in shape and in magnitude, on the potential at the nuclear surface. It is therefore important to match the optical potential with the wave functions in the mentioned region; i.e., to calculate this potential using the nuclear density as obtained from the actual nuclear wavefunctions.

Another aspect which, in calculations of the optical potential from nucleon–nucleon cross sections, has not been taken into account up to now in the case of quasi-free scattering [except in (GB71)], is the effect of the Pauli principle on the nucleon–nucleon scattering inside nuclei.[1] As is well known, the effect of the exclusion principle is to increase the mean free path of the nucleons inside nuclear matter, especially at relatively low energies (Go48, LMT59, DS63): the resulting effective proton–nucleon cross section is constant within 20% inside nuclear matter of normal density between about 80 MeV and 800 MeV. This has been verified through the analysis of elastic proton–carbon scattering (Ba61, Fa71).

The experimental results for the p state of ^{12}C, given in Fig. 1, show that the magnitude of the distorted momentum distribution for $(p, 2p)$ reactions is indeed not very dependent on energy between 160 and 1000 MeV incident energies. Neglecting the Pauli principle, one would obtain a much lower quasi-free cross section for incoming energies of about 160 MeV than for those at 300 or more MeV due to the larger absorption of the outgoing protons. For relatively low energies, it might even be advisable to take the density dependence of the correction due to the Pauli principle into account; this will result in an energy dependence of the shape of the imaginary part of the optical potential.

We now direct ourselves to another problem, namely that of how to represent practically the results obtained in $(p, 2p)$ experiments. Because of the increasing use which is being made of the kinematical degrees of freedom of the reaction, this is not a trivial problem.

The distorted momentum distribution $\sum|g'|^2$ has, in the distorted wave impulse approximation, the

[1] We thank A. F. de Toledo Piza for an interesting discussion of this point.

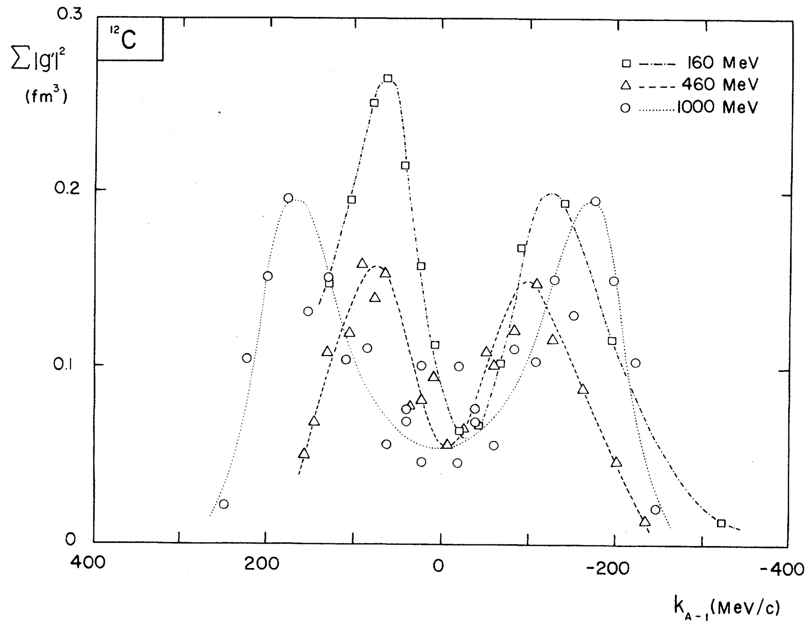

FIG. 1. Distorted momentum distributions for the $1p$ state of ^{12}C obtained from $(p, 2p)$ experiments at three different energies; the lines drawn through the experimental points are meant only as guides for the eye. The data for the three energies have been taken from (GWS67), 160 MeV; (TKS+66), 460 MeV; (SFP+70), 1000 MeV.

form (MHT58)

$$\sum|g'|^2=(2J_A+1)^{-1}\sum|\int\exp(i\mathbf{k}_{A-1}\cdot\mathbf{r})\times\prod_{i=0}^{2}D_i(\mathbf{r})\psi_{J_AM_A}(\mathbf{r})\,d^3r\,|^2, \quad (2.1)$$

where $\psi_{J_AM_A}(\mathbf{r})$ represents, in general, the overlap integral (hole wave function). For a detailed study of the general properties of the overlap integral we refer to (Be65). The distorting functions $D_i(\mathbf{r})$ are, in the WKB approximation, given by

$$D_i(\mathbf{r})=\exp[-i(E_i/\hbar^2c^2k_i)\int V_i(\mathbf{r}')\,ds_i]. \quad (\mathrm{I}3.32)$$

If distortion is neglected $[D_i(\mathbf{r})\equiv1,\ i=0,\ 1,\ 2]$, $\sum|g'|^2$ is only dependent on $|\mathbf{k}_{A-1}|$. However, in general the $D_i(\mathbf{r})$'s are very much different from unity and not spherically symmetric, as well as being dependent on the geometry of the experiment.

In the following we shall limit ourselves to coplanar experiments, in which the angles and energies of the outgoing protons are not *very* different from the ones of a symmetric scattering on protons at rest. Because the external momenta involved at the energies considered are in general very much larger than the internal momenta in the nucleus, it will be possible to scan the nucleon momentum distributions keeping this condition of an approximately symmetric geometry. The higher the incoming energies, the better this geometrical requirement can be fulfilled; in fact, it is met rather well in most experiments which have been performed at the energies considered.

Under the above condition one expects from formula (I3.32) that, to a reasonable approximation, the change in $\prod_iD_i(\mathbf{r})$ caused by the relatively small changes in the geometry (parametrized by some choice of a third parameter which is still free) can be neglected; i.e., that one can neglect the implicit dependence of $\prod_iD_i(\mathbf{r})$ on $\mathbf{k}_{A-1}$. This point was first noted in (GWS67) and, as will be seen in Sec. 3, several experiments exist which confirm this expectation.

Under these circumstances, in Eq. (2.1) the only essential dependence on the recoil momentum remaining in $\sum|g'|^2$ is that through $\exp(i\mathbf{k}_{A-1}\cdot\mathbf{r})$. The momentum $\mathbf{k}_{A-1}$ is parallel to the scattering plane because of the assumed coplanarity. It would therefore appear useful to plot the experimental results as contour diagrams of $\sum|g'|^2$ in a two-dimensional $\mathbf{k}_{A-1}$ graph. Of course, one effect of the factor $\prod_iD_i(\mathbf{r})$ is to destroy the rotational symmetry in such a graph.

Let us suppose that the contour diagrams mentioned have been determined for a fixed excitation energy of the final nucleus at several bombarding energies between, say, 150 and 1000 MeV, and let us discuss the effect of a change in energy on this diagram. From Eq. (2.1) one sees that the energy dependence of $\sum|g'|^2$ is contained only in the distorting factors $D_i(\mathbf{r})$. Separating the real and imaginary parts of the optical potentials in the exponent of Eq. (I3.32), one observes that the changes in the real parts resulting from the energy variation will give (approximately) a phase factor of the type $\exp(i\mathbf{\Delta k}\cdot\mathbf{r})$. The vector $\mathbf{\Delta k}$ has the direction of the incident proton (because of the assumed approximate symmetry) and can be expressed in the changes of the real parts of the distorting optical potentials. The description of the same effect in coordinate space has been given in a recent interesting paper (GB71).

On the other hand, the imaginary parts of the optical potentials result in a real factor in the $D_i(\mathbf{r})$'s. This factor is smaller than unity and is expected to be only slightly energy dependent, because, as discussed above, the absorption is nearly constant with energy.

To summarize, one would expect the contour diagrams at various energies to be *shifted* by an amount approximately $\Delta k(E_0)$ along the direction of the momentum of the incident proton and to have a slightly varying over-all normalization. The experimental confirmation of such a behavior would considerably strengthen one's confidence in the quantitative treatment of the reaction and consequently give the nuclear structure information extracted from quasi-free data a stronger basis.

The dependence of $\sum |g'|^2$ on the direction the recoil momentum makes with the incident direction has been measured at 600-MeV incident energy (KLR+71) and will be discussed in Sec. 3.1a. Interesting calculations using the distorted wave impulse approximation, which qualitatively reproduce the experimental variation of $\sum |g'|^2$, have been performed for shell model states in ^{12}C and ^{40}Ca (KLR+71) and in ^{28}Si (KLR+71, GB71).

To conclude this section on the reaction mechanism, we briefly discuss "off energy-shell" effects, which are of interest in the interpretation of some of the quasi-free measurements.

As was remarked in I [p. 128; see also (MHT58)], the use of the free proton–proton cross section in formula (I3.31) has an arbitrary feature due to the fact that the set of momenta occurring in quasi-free scattering does not occur in any free scattering process, because of the energy absorbed by the residual nucleus. This off energy-shell effect has been quantitatively studied (RSL70, SRLH72). The conclusion is the same as that in I, namely, that it is for all present purposes a good approximation to take the free elastic proton–proton cross section at the equivalent center of mass energy, if this energy falls in the range in which the free proton–proton cross section is almost independent of energy and angle, i.e., 150–500 MeV. This means that, for bombarding energies at the lower or higher limits of this range, Eq. (I3.31) becomes unreliable for certain kinematical configurations of the outgoing protons where the equivalent free proton–proton cross section is sensitively dependent on the choice of the off-shell extrapolation process. A definite proposal is made in (RSL70) for this extrapolation, but arguments for other procedures can also be advanced.

Consider for example a symmetric $(p, 2p)$ process in the model in which a bound proton with binding energy B is knocked out from a square well potential $(-|V|)$ which also operates on the incoming and outgoing protons. The potential well is supposed to be sufficiently extended so that surface effects can be neglected. The total energy of the outgoing proton would be an amount $-B$ "off-shell." To obtain the impulse approximation of the process in this model it is evident that one should simply take the "on-shell" matrix element for an incoming energy $E_0+|V|$, E_0 denoting the actual incoming energy. It would therefore be incorrect to make any off-shell extrapolation of the two body scattering matrix element, as naively would be suggested by the missing energy B.

It seems therefore that kinematical situations in which the choice of an extrapolation procedure becomes important should be avoided in a calculation of the distorted momentum distribution. The values of the separation energies are, of course, not affected by this uncertainty. From this discussion it appears impossible to learn anything about the off-shell matrix elements relevant to the two particle system from those of $(p, 2p)$ reactions without taking the precise mechanism causing the "off-shellness" for this last case into account.

In the quasi-free electron–proton processes one can correct for the off energy-shell effect because in this case the Born approximation is in general valid and one can analytically continue the extensively studied proton form factors. However, for such electron experiments one still has, except in special kinematical situations, the uncertainty of whether the embedment of the proton in nuclear matter has a negligible influence on these form factors. We will return to this problem in Sec. 4.

2.2 Final Nuclear States

With respect to the final nuclear states, the approximation of the overlap integrals occurring in Eq. (I3.31) by single-particle states is a simple but in many cases also a poor approximation. This was in fact recognized from the very beginning, but as this and related points have come up repeatedly in the recent literature, we make a few remarks on the formation of the final hole state.

In a quasi-free experiment, a hole state is created whose energy is determined by the choice of the energies of the incoming and outgoing protons. If the energy of this state lies in the discrete part of the energy spectrum of the residual nucleus, the process can occur only at discrete energies. If the energy of the process is chosen to be in the continuum part, the process is possible at all energies. However, at certain energies of the residual nucleus the lifetime of the hole may be exceptionally large. These energies correspond to the peaks in the spectrum. One may consider these peaks as caused by a decaying hole or as caused by a superposition of stationary continuum states, both interpretations being equivalent (TMH57).

Those hole states which immediately decay contribute to the continuous background in the spectrum. It is clear that short-range correlations play an important role here, because if a particle is knocked out, another one which is just colliding with it will have the tendency to be excited or ejected also.

All the contributions mentioned up to now are included in the expression (I3.31). This is not so for certain other, experimentally indistinguishable, events, namely the contributions of the protons which are multiply scattered before or after a quasi-free process. This background is quite different for $(p, 2p)$ and $(e, e'p)$ processes. From the size of the reduction factors of the quasi-free processes it is clear that in the $(p, 2p)$ case the total integral of this background may be an order of magnitude larger than that over the quasi-free contributions. In the $(e, e'p)$ case, both integrals will be of the same order of magnitude. Fortunately the multiple scattering background is likely to be smooth, to be displaced to excitation energies higher than the ones of the stationary and quasi-stationary peaks and to be spread over a large angular range (I).

This simple picture shows the difficulties connected with the testing of any sum rule which is based on the single particle character of the transition (Ko72). In practice one cannot take the short lived hole states of the continuous background into account, because this extends to very high energies. And if one did so, the large unwanted multiple scattering contributions would have been included.

Recently it was remarked (MP71, BMP72) that the ability of the final nucleus to re-arrange during the scattering process will be dependent on energy, the two extreme cases being the adiabatic and the sudden removal of a nucleon. This will cause an energy dependence of the shape of the spectrum. Connected with this problem is an interesting calculation (PA72) of the influence of the outgoing protons on the decaying hole states. The point is that the multiple scattering can lead to states which are coherent with those resulting from the short lived hole states, i.e., the two fast particles to be observed are with an appreciable probability still inside the nucleus when it decays (Co65, Am67). The calculations (PA72) indicate that the resulting deformation of a broad peak in the spectrum is significant though not large.

It is possible to write the angular correlation distribution occurring in Eq. (I3.31) in an elegant way, which is particularly instructive for the case of a hole in a strongly bound shell (GL70). Using the Heisenberg representation, one may express the overlap integral as the matrix element of a proton annihilation operator $a(\mathbf{x}, t)$ between the ground state of the initial nucleus and the considered final state of the residual one:

$$\begin{aligned} g_f(\mathbf{x}) &= \int \psi_f^*(\mathbf{x}_1, \cdots, \mathbf{x}_{A-1}) \psi_i(\mathbf{x}, \mathbf{x}_1, \cdots, \mathbf{x}_{A-1})\, d^3x_{A-1} \\ &= \langle f \mid a(\mathbf{x}) \mid i \rangle, \end{aligned} \tag{2.2}$$

with $a(\mathbf{x}) = a(\mathbf{x}, t=0)$. For the distorted momentum distribution, this gives

$$\begin{aligned} g_f'(\mathbf{k}) &= \int \exp(i\mathbf{k}\cdot\mathbf{x}) \prod_j D_j(\mathbf{x}) \langle f \mid a(\mathbf{x}) \mid i \rangle\, d^3x \\ &= \int [\![\prod_j D_j]\!](\mathbf{k}-\mathbf{p}) \langle f \mid a(\mathbf{p}) \mid i \rangle\, d^3p, \end{aligned} \tag{2.3}$$

where $[\![\prod_j D_j]\!](\mathbf{k}-\mathbf{p})$ and $a(\mathbf{p})$ are the three-dimensional Fourier transforms of $\prod_j D_j(\mathbf{x})$ and $a(\mathbf{x})$.

Up to a constant factor one may therefore write

$$\begin{aligned} \sum_f \mid g_f'(\mathbf{k}) \mid^2 \delta(E_f - E_i - E_S) &= \int d^3p\, d^3p' \\ &\times [\![\prod_j D_j]\!](\mathbf{k}-\mathbf{p}) \sum_f \mid \langle i \mid a^\dagger(\mathbf{p}') \mid f \rangle \\ &\times \delta(E_f - E_i - E_S) \langle f \mid a(\mathbf{p}) \mid i \rangle \mid [\![\prod_j D_j^*]\!](\mathbf{p}'-\mathbf{k}), \end{aligned} \tag{2.4}$$

where E_f and E_i are the energies of the final and initial nucleus, respectively, and E_S is the separation energy.

On the other hand, we have for the retarded hole two point function

$$\begin{aligned} -iG^H(\mathbf{p}, t; \mathbf{p}', 0) &= \langle i \mid a^\dagger(\mathbf{p}, t) a(\mathbf{p}', 0) \mid i \rangle \theta(t) \\ &= \sum_f \langle i \mid a^\dagger(\mathbf{p}, t) \mid f \rangle \\ &\qquad \times \langle f \mid a(\mathbf{p}', 0) \mid i \rangle \theta(t) \\ &= \sum_f \exp[i(E_i - E_f)t] \\ &\times \langle i \mid a^\dagger(\mathbf{p}, 0) \mid f \rangle \langle f \mid a(\mathbf{p}', 0) \mid i \rangle \theta(t), \end{aligned} \tag{2.5}$$

and consequently

$$\begin{aligned} \int \exp[i(\omega + i\epsilon)t] G^H(\mathbf{p}, t; \mathbf{p}', 0)\, dt &= \sum_f (E_f - E_i - \omega - i\epsilon)^{-1} \\ &\times \langle i \mid a^\dagger(\mathbf{p}) \mid f \rangle \langle f \mid a(\mathbf{p}') \mid i \rangle. \end{aligned} \tag{2.6}$$

The corresponding Källén–Lehmann spectral density is defined by

$$\begin{aligned} \rho^H(\mathbf{p}, \mathbf{p}', \omega) &= \operatorname*{Im}_{\epsilon\to 0} \int \exp[i(\omega + i\epsilon)t] \\ &\qquad \times G^H(\mathbf{p}, t; \mathbf{p}', 0)\, dt \\ &= \pi \sum_f \delta(E_f - E_i - \omega) \langle i \mid a^\dagger(\mathbf{p}) \mid f \rangle \\ &\qquad \times \langle f \mid a(\mathbf{p}') \mid i \rangle. \end{aligned} \tag{2.7}$$

Inserting this expression in Eq. (2.4), one finds

$$\begin{aligned} \sum_f \mid g'(\mathbf{k}) \mid^2 \delta(E_f - E_i - E_S) &= \int d^3p\, d^3p' \\ \times [\![\prod_j D_j]\!](\mathbf{k}-\mathbf{p}) \rho^H(\mathbf{p}, \mathbf{p}', E_S) [\![\prod_j D_j^*]\!](\mathbf{p}'-\mathbf{k}). \end{aligned} \tag{2.8}$$

Formally it is simpler to replace ρ^H by the spectral density of the full fermion Green's function (the T product of the a's), because this quantity occurs naturally in perturbation theory and the particle part thus added does not contribute at those values of E_S relevant for the present purpose.

For a clear discussion of the connection of this propagator with the properties of single-particle and single-hole states and for references to the original works we quote the book (FW71), in particular Sec. 7;

one finds there also a review of the relation between the complex energies for which the propagator has poles on the unphysical Riemann sheet and the energies and widths of the quasi-stationary single-particle and single-hole states.

The present formalism is taken from relativistic quantum field theory, where the holes correspond to antiparticles. In that case, if charge conjugation invariance is assumed, the spectra of holes and particles are identical. In the nuclear case, such a symmetry between particles and holes is only very approximately present and therefore the properties of single hole excitations are rather different (though not completely so) from the ones of single particles (GB60).

Because one is dealing with hole states, "discrepancies" between experimentally determined excitation energies or momentum distributions and theoretical calculations based on single-particle approximations should not be too surprising. A many-body calculation of the energy corrections to be expected in such an approximation, giving the "rearrangement energies" and the widths, has been performed (Kö66) and the calculated widths have the correct order of magnitude. For very heavy nuclei, widths corresponding to those of nuclear matter might be expected, but it is interesting to observe that the calculated widths for the strongly bound states are nearly independent of the mass number even for relatively light nuclei.

The same effect has been observed (HFG71) in the results of a resonance model calculation of the decay width for inner shells of light nuclei. Another recent calculation (BP70, Be72) of the splitting of the $1s$ hole state by the coupling with degenerate states gives a reasonable agreement with the overall experimental width of the $1s$ state in ^{16}O.

Assuming that the distortion can be approximated by a suitable constant reduction factor d, which is a quite good approximation for $(e, e'p)$ processes provided the outcoming proton has an energy between 150 and 500 MeV (JM62, EG70, At71), one has

$$[\![\prod_j D_j]\!](\mathbf{k}-\mathbf{p})=d\delta^3(\mathbf{k}-\mathbf{p}) \qquad (2.9)$$

and Eq. (2.8) becomes

$$\sum_f |\, g_f'(\mathbf{k})\,|^2\, \delta(E_f-E_i-E_S)=d^2\rho^H(\mathbf{k},\mathbf{k},E_S). \qquad (2.10)$$

This equation has been used (WGL71, Wi71, WL72) as the basis for calculations in which the Dyson equation obeyed by the full propagator for the cases of ^{12}C and ^{16}O was approximately solved; however the calculated energy spectra do not agree with the experimental ones, both with respect to the widths and to the positions of the peaks (of course taking experimental resolutions into account). For a recent discussion along similar lines of the problems of energies, widths, wave functions, and spectroscopic factors we refer to (EW72).

The main features of the experimental results on the energies and widths of hole states (Fig. 11 below) show a tendency to vary little from one nucleus to the neighboring ones. In order to obtain a simple zero-order description of hole states over a large range of nuclei, it is therefore tempting to follow the shell model approach by considering the hole as being bound by a suitable potential which varies smoothly with atomic number. As in the shell model, this hole potential could be somewhat state dependent, but should be taken to be complex in this case. Its eigenstates with complex eigenvalues describe, respectively, the wave functions, energies, and widths of the quasi-stationary hole state (HJM68). Estimates in such a model, in particular of the influence of the finite lifetime on the momentum distributions of the hole, have been performed in (He71), by solving the Schrödinger equation for several complex potentials in an approximate way. In these calculations the real potential was taken as a usual single-particle potential, and various types of imaginary potentials were chosen *ad hoc*, but normalized so as to reproduce the observed widths of the hole states. As expected, the addition of this imaginary potential can have a considerable influence on the momentum distributions, and this influence is strongly dependent on the shape of the imaginary potential.

To obtain a better insight into the effective hole potential, it might be of interest to calculate the complex hole state potentials in nuclear matter (Kö66) for different densities and binding energies and then to use these potentials in a "local approximation" for calculations of the type performed in (He71). However, it may well be that the holes in finite nuclei are strongly coupled to surface vibrations, which may have comparable excitation energies. This could demand a modification of the effective complex potentials obtained from nuclear matter calculations[2] by a surface term.

These problems are far from clear, but the attempt to obtain some general insight into single-hole states from the situation in nuclear matter seems to us, at the present stage, an attractive alternative to detailed level scheme calculations in specific nuclei.

Finally, we make a brief remark on the calculation of fractional parentage coefficients, which, if we neglect the absorption and consider the case in which the proton is knocked out of a loosely bound shell, will govern the relative intensity distribution in the energy spectra. For example, in a pure L–S model the knock-out of a $1p$ proton from ^{12}C should result (THM58) in $\frac{1}{2}^-$ and $\frac{3}{2}^-$ states of ^{11}B with an intensity ratio of 1:2. It is however clear that the neglect of the relative differences in the large absorptions cannot be a good approximation for the case of $(p, 2p)$ processes even in a nucleus as light as ^{12}C.

[2] We are thankful to A. Bohr, G. E. Brown, D. H. E. Gross, and B. Mottelson for an interesting discussion on this point.

Table I. $(p, 2p)$ and $(e, e'p)$ coincidence experiments with incident energies larger than 100 MeV on nuclei with $A \geq 4$, performed after 1966 (complementary to Table I of I).

Group	Type of experiment	Energy	Nuclei investigated
Brookhaven[a]	Asymmetric $(p, 2p)$	1000 MeV	^{12}C
CERN[b]	Asymmetric $(p, 2p)$	600 MeV	^{12}C, ^{28}Si, ^{40}Ca, ^{51}V, ^{90}Zr
Harvard[c]	Asymmetric $(p, 2p)$	160 MeV	^{12}C
Liverpool[d]	Asymmetric $(p, 2p)$	385 MeV	^{12}C, ^{40}Ca, ^{45}Sc, ^{59}Co, ^{58}Ni, ^{120}Sn, ^{208}Pb, ^{209}Bi
Orsay I[e]	Symmetric $(p, 2p)$	156 MeV	^{6}Li, ^{7}Li, ^{9}Be, ^{23}Na, ^{24}Mg, ^{28}Si, ^{40}Ca, ^{45}Sc, ^{48}Ti, ^{51}V, ^{52}Cr, ^{55}Mn, ^{56}Fe, ^{59}Co, ^{58}Ni, ^{64}Zn, ^{75}As, ^{90}Zr
Orsay II[f]	Noncoplanar $(p, 2p)$	≤ 110 MeV	^{12}C
Rome[g]	Asymmetric $(e, e'p)$	580–750 MeV	^{12}C, ^{40}Ca, ^{75}As
Saclay[h]	Asymmetric $(e, e'p)$	500 MeV	^{12}C, ^{28}Si, ^{40}Ca, ^{58}Ni
Tokyo[i]	Asymmetric $(e, e'p)$	700–750 MeV	^{6}Li, ^{7}Li, ^{9}Be, ^{12}C, ^{27}Al, ^{40}Ca, ^{51}V
Virginia[j]	Symmetric $(p, 2p)$	600 MeV	^{4}He

[a] (SFP+70).
[b] (KRF+71), (LYK+71), (KLR+71).
[c] (GWS67).
[d] (JABCL69), (JAKL69).
[e] (RAD+67), (RAJ+67), (ADRRR67).
[f] (YH67).
[g] (ACC+66a), (ACC+66b), (ACC+67), (CCC+72).
[h] (BMHPS71), (ABD+72).
[i] (HKM+70), (HKM+72).
[j] (PSG+69).

Furthermore, even in cases in which we believe we have a good knowledge of the spectroscopic factors as, e.g., for the p states of ^{16}O, and in which distortion is taken as well as possible into account, one is not able to obtain good agreement between theoretical calculations (Ma58/59, BJ63, TKS+66) and experimental results obtained in $(p, 2p)$ scattering. But in almost all calculations of spectroscopic factors (e.g., KS67, JJ67, At68, Jai68, BKM69, KS69, Ja71) either distortion has been completely neglected or only crudely taken into account. It seems therefore clear that one can not yet rely on the detailed values of the spectroscopic factors derived from this type of experiments.

3. EXPERIMENTAL RESULTS

Since the publication of I, much progress has been made in the experimental aspects of quasi-free scattering. The $(p, 2p)$ experiments have been extended to higher energies (up to 1 GeV), to some of the heavier nuclei (up to $A=209$), and to other geometries. In quasi-free electron scattering the first angular correlation distributions have been determined and very recently experiments with good energy resolution were performed. The new experiments are listed in Table I.

In this section some typical new results will be discussed and a summary of the available information will be given.

3.1 Quasi-Free Proton Experiments

3.1a Distorted Momentum Distributions

The effect of varying some of the many degrees of freedom existing in the $(p, 2p)$ experiments (departing from the symmetric situation, see I, p. 123) has been studied at different energies. As mentioned in Sec. 2.1, most of the experiments (GWS67, JABCL69, JAKL69, SFP+70, KRF+71, LYK+71) have been performed in such a way as to include and not depart too strongly from the symmetric geometry. Besides the momentum $\mathbf{k}_{A-1}$ in the scattering plane, the third (free) parameter mentioned in Sec. 2.1 has been taken as the energy sharing parameter $x^2=T_1/T_2$ $(T_2 \geqslant T_1)$ in the Harvard (GWS67) experiment (160 MeV) and in the Brookhaven (SFP+70) experiment (1 GeV), as the momentum of one of the outgoing protons $|\mathbf{k}_1|$ in the Liverpool (JABCL69, JAKL69) experiment (385 MeV), and as the angle of one of the outgoing protons θ_1 in the CERN (KRF+71, LYK+71) experiment (600 MeV).

For these coplanar experiments, a two-dimensional contour diagram of $\sum |g'|^2$, showing the variation with the recoil momentum vector $\mathbf{k}_{A-1}$, would be very interesting. The published results of the various experiments have been presented in another way, namely by calculating the momentum distributions over certain

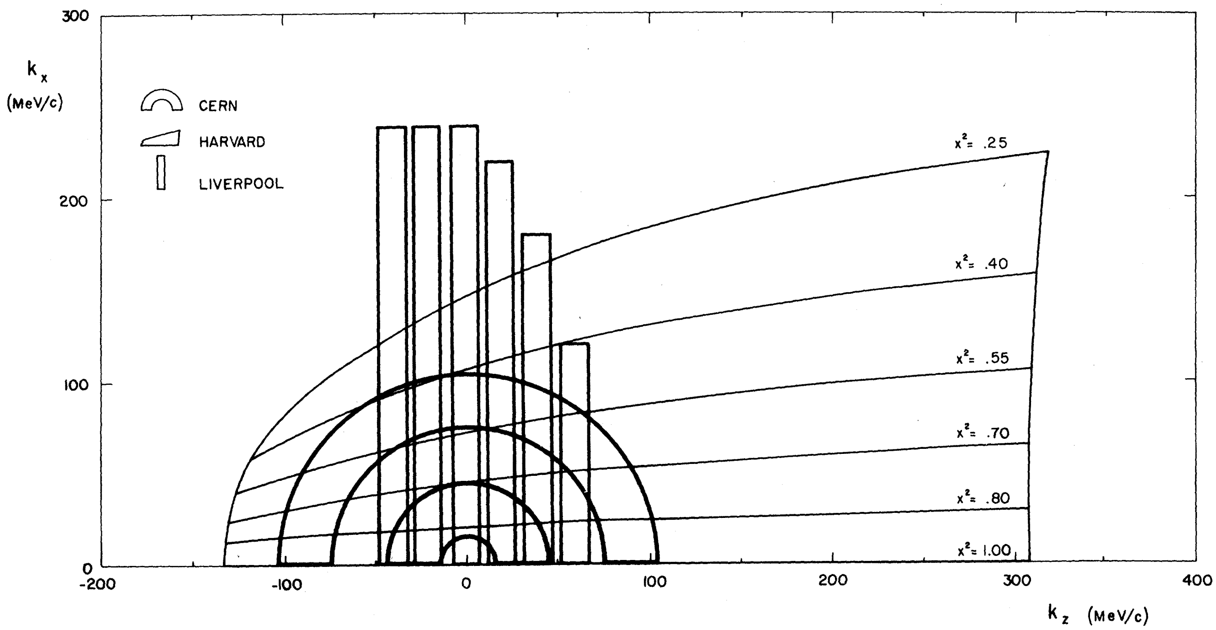

FIG. 2. Strips in momentum space along which the variation of momentum distributions with the components of the momentum have been presented for the various (p, $2p$) experiments on ^{12}C.

strips in the two-dimensional **k** plane; the type of contours followed in the different experiments on ^{12}C are indicated in Fig. 2. Of course for the symmetric experiments ($|\mathbf{k}_1|=|\mathbf{k}_2|$, $\theta_1=\theta_2$), the covered region reduces to the k_z axis. Unfortunately it is not quite possible to construct a good contour diagram from the published data.

As there are available only the four mentioned experiments, in which $\sum|g'|^2$ is measured off this k_z axis, and because rather different parameters have been used in each of them, we briefly discuss each measurement separately.

In the Harvard experiment (regions shown in Fig. 2 by thin lines), the angles of the two outgoing protons have been kept equal, and angular distributions have been measured for different values of x^2 for the $1p$ and the $1s$ state of ^{12}C, the incident energy being 160 MeV. Figure 3 shows the results for $\sum|g'|^2$ for both the $1s$ and the $1p$ state. As stressed in (GWS67) and as remarked in Sec. 2.1, this function of $|\mathbf{k}_{A-1}|^2$ is independent of the third parameter over a remarkably large range.

The result of the 1 GeV Brookhaven experiment for the $1p$ state of ^{12}C, shown in Fig. 1, has approximately

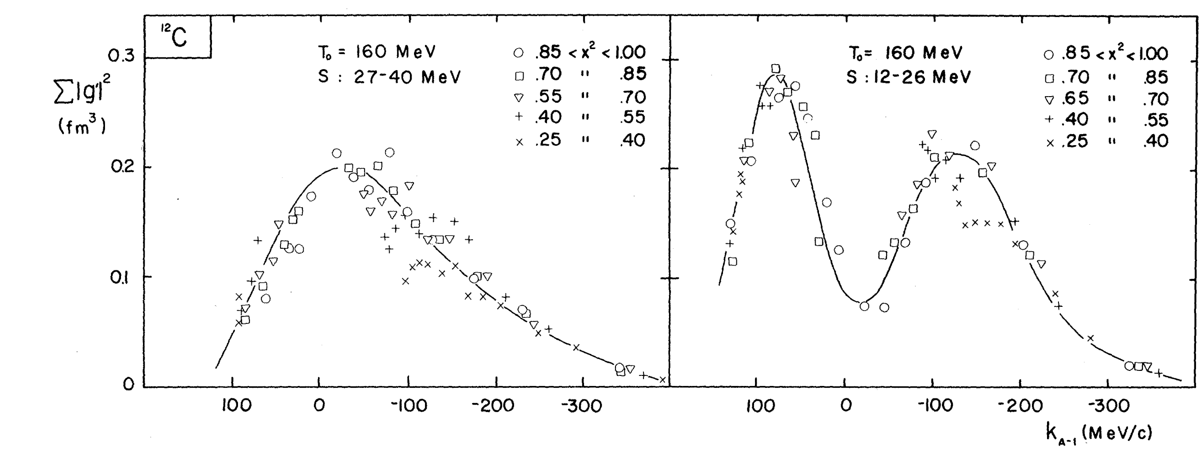

FIG. 3. Distorted momentum distributions for the $1s$ and $1p$ states of ^{12}C at various sharing parameters $x_2=T_1/T_2$, the incident energy being 160 MeV; the lines are meant to guide the eye through the experimental points. The independence of the distorted momentum distribution on the individual energies of the outgoing protons is clearly shown [From (GWS67)].

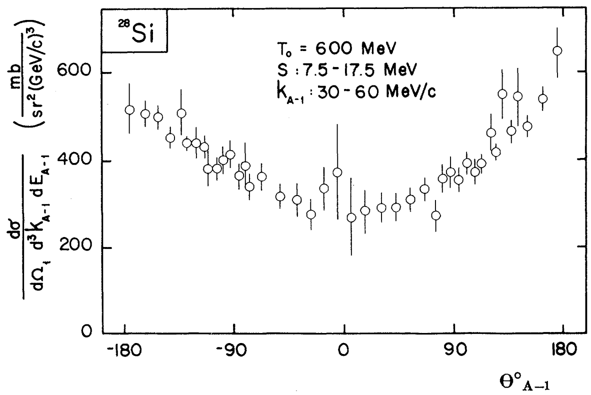

FIG. 4. Variation of the $(p, 2p)$ cross section for the $2s$–$1d$ states of ^{28}Si with the angle between the recoil momentum and the incident beam [from (KLR+71)].

the same magnitude as that at 160 MeV as remarked in Sec. 2.1.

In the Liverpool experiment which was performed at 385 MeV, the third parameter was taken to be the momentum of one of the outgoing protons $|\mathbf{k}_1|$. As in the experiment at 160 MeV, it was shown that the distorted momentum distribution is practically independent of this third parameter. Distorted momentum distributions have been plotted for coplanar momenta orthogonal to the incident momentum (medium thick lines in Fig. 2). Results for several nuclei have been obtained, showing evidence for many shell model states; we will give details on these measurements in Sec. 3.1b.

The most recent experiment, in which the various degrees of freedom in the $(p, 2p)$ reactions have been exploited, is that performed at CERN with an incident energy of 600 MeV. The third parameter has been taken as the angle, θ_1, which one of the outgoing protons makes with the incident beam; it was again shown that the angular correlation distribution is rather independent of this extra variable.

In this experiment, for the first time the variation of the correlation cross section with the recoiling angle of the residual nucleus was studied for various excitation energies and for several nuclei, keeping the incoming energy, the excitation energy, and the absolute value of the recoil momentum fixed. For ^{12}C, the strips covered in the published results are indicated by the thick lines in Fig. 2. As an example of such measurements, the case of the $2s$–$1d$ states in ^{28}Si is given in Fig. 4. It has been observed (KLR+71) that, in general, the $1s$ states have the smallest variation with the recoil angle. This is understandable because the $1s$ momentum distribution is concentrated mainly around the zero momentum value (at zero momentum, of course no variation with θ_{A-1} exists).

The Virginia group (PSG+69) measured the distorted momentum distribution of ^{4}He at 600 MeV incident energy using a symmetric geometry; measurements were made up to a relatively high momentum transfer (300 MeV/c), and the results agree with earlier ones (TKS+66).

To conclude this section, we mention the only systematic noncoplanar measurements performed thus far (YH67). This interesting and difficult experiment, designed to investigate the diffraction effects due to scattering in the two pole caps of the target nucleus, has been performed at relatively low incident energies ($\leq$110 MeV). Although the results show some maxima and minima, more data are needed to establish predicted interference effects (JM60, PB72).

3.1b Energy Spectra

In recent years the $(p, 2p)$ experiments have been extended to higher energies and larger A, and a new way of obtaining the energy spectra has been devised. The new experiments are listed in Table I, which is thus complementary to Table I of I. A general summary of the results will be given in Sec. 3.3.

The new way of analyzing the data was first used in the Liverpool experiments (385 MeV). In these measurements, angular correlation distributions were determined at fixed energy intervals (mostly 5 MeV) and the structure of these distributions analyzed with (plane wave) harmonic oscillator momentum distributions of adjustable normalization. This means that the change of shape of the momentum distributions due to distortion is neglected, and the absorption is given by a reduction factor determined so as to fit the experimental results. In such a way, use has been made of the variation of the angular distribution with excitation energy. Even if the energy spectrum at each angle does not show a pronounced structure, one may find the contributions of the various shells by decomposing the momentum distributions at a fixed energy in, e.g., harmonic oscillator momentum densities. The coefficient with which each harmonic oscillator density function contributes to the cross section was plotted in this Liverpool experiment as a function of energy. This procedure is shown in Fig. 5 for ^{40}Ca; the results obtained in the same way for several other nuclei are given in Fig. 6. One should however still consider the results for the very deep shells in medium light nuclei with some reservation until they have been confirmed by $(e, e'p)$ experiments, because their small contributions in the energy spectrum might be difficult to distinguish from a possible structure in the multiple scattering background[3] (see also Sec. 4).

In the CERN experiment (600 MeV), this type of analysis has been improved in that experimentally determined distributions $\sum |g'|^2$ were used instead of the harmonic oscillator momentum densities. The results for ^{40}Ca were confirmed and the hole states expected in ^{28}Si from the shell model description of nuclei observed. Figure 7, showing the energy spectrum for

[3] We thank J. S. Blair for an interesting discussion of this point.

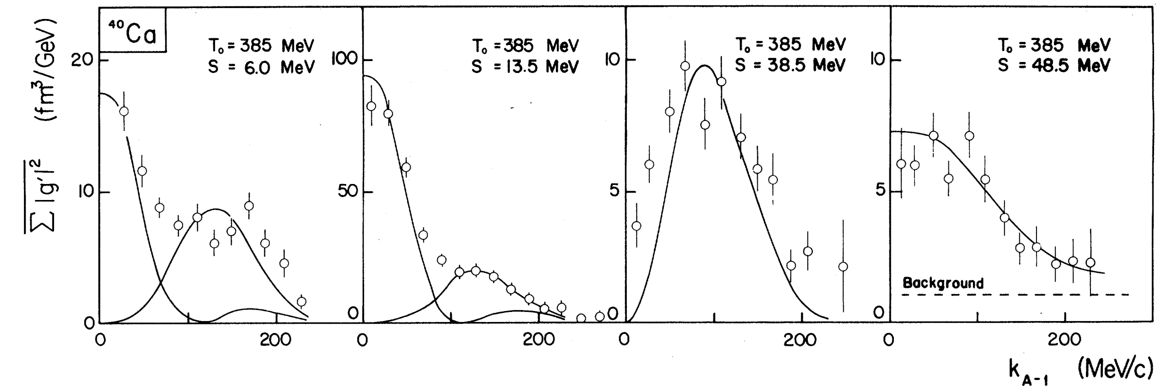

FIG. 5. Distorted momentum distributions of the various states in ^{40}Ca, obtained from $(p, 2p)$ reactions at an incident energy of 385 MeV. The full lines show the decomposition of the distorted momentum distributions in harmonic oscillator momentum densities [from (JAKL69)].

^{28}Si at small momentum transfer, strikingly exhibits both the 1*s* and the 2*s* state in this nucleus; in Fig. 7 also the momentum distributions of the deep lying 1*p* and 1*s* hole states are shown.

Several 1*p*, 2*s*–1*d*, and 2*p*–1*f* shell nuclei have been investigated with improved energy resolution (up to 1.7 MeV), using a symmetric geometry at incident energies of 156 MeV, by the Orsay group (RAD+67, RAJ+67, ADRRR67). In these interesting experiments many upper shell states have been identified and some inner shell states have been detected; in some cases a fine structure in these inner shell states has been observed. In particular, the 2*s* hole state has been followed up for several 1*f* shell nuclei.

3.2 Quasi-Free Electron Experiments[4]

The new quasi-free electron experiments, listed in Table I, have been performed with the synchrotrons in Frascati and Tokyo and with the linear accelerator in Saclay. The measured energy spectra and angular correlations in general show structures which are comparable to the ones observed in the $(p, 2p)$ experiments. It seems clear that the final aim should be an analysis similar to the one applied to the Liverpool and CERN

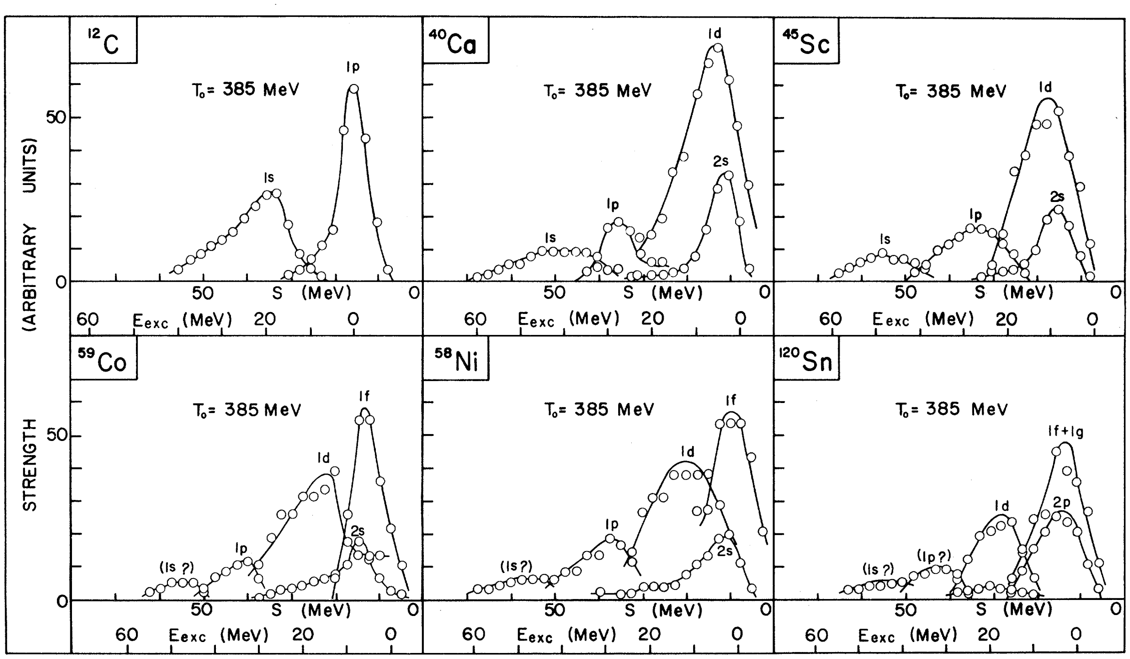

FIG. 6. Strength of shell model states in several nuclei, resulting from decompositions of the distorted momentum distributions as shown in Fig. 5, obtained from $(p, 2p)$ reactions at an incident energy of 385 MeV [from (JABCL69) and (JAKL69)].

[4] As the results of (CCC+72, ABD+72, HKM+72) were received after submission of the manuscript, it was not possible to include these data in the figures.

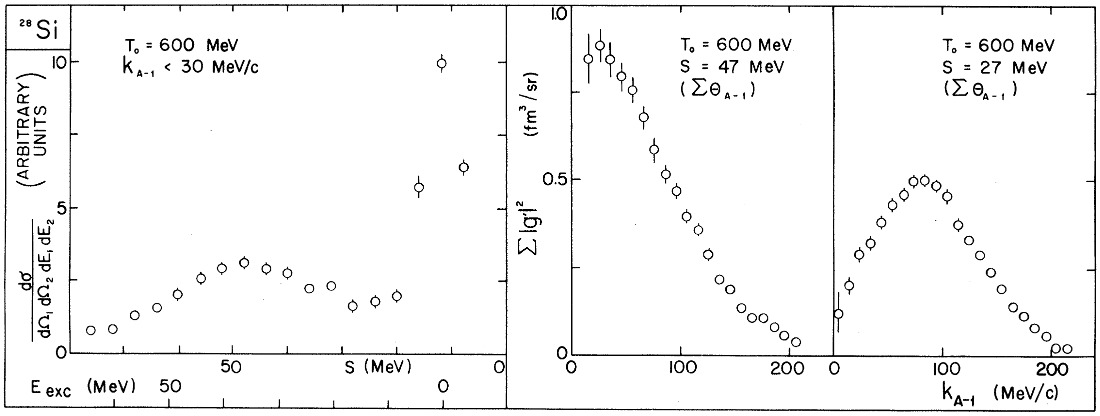

Fig. 7. Energy spectrum (at low recoil momentum) and distorted momentum distributions of the $1p$ and $1s$ states in ^{28}Si, obtained through $(p, 2p)$ reactions at an incident energy of 600 MeV [from (KRF+71) and (LYK+71)].

experiments through the measurement of angular correlations as a function of separation energy. If such measurements could be performed with sufficient statistics, a detailed knowledge of the practically undeformed momentum distributions of the quasi-stationary hole states might be obtained. We briefly discuss the various new experiments which represent encouraging steps in this direction.

In Frascati, the Sanità group (Rome) has measured, with varying incoming energy (580–750 MeV) and a resolution of about 10 MeV, spectra of ^{40}Ca (ACC+66a) and ^{75}As (ACC+66b), which show indications of maxima and minima.

This group has also measured the first angular correlations (ACC+67); the results for 16 MeV and 35 MeV separation energies in ^{12}C, corresponding to the $1p$ and $1s$ shells, are given in Fig. 8 and indeed show the typical behavior expected for these shells. The attempt to explain these data with the same parameters used in the analysis of elastic electron scattering has stimulated several calculations (At68, BPS68, Wa68, BBAS68, EG70, SJ71, Ra72a, Ra72b). In ^{40}Ca, angular correlations have been measured (CCC+72) for 39 MeV and 81 MeV separation energies. The 39-MeV data clearly exhibit the expected p state behavior. Surprisingly, the 81-MeV distribution is quite comparable to the presumably $1s$ state behavior observed around 50 MeV in $(p,2p)$ measurements in this nucleus (JAKL69, LYK+71). Before drawing further conclusions from this measurement, the still necessary experimental and theoretical corrections should be taken into account.

The first experiments in Tokyo (HKM+70) at 750 MeV with a resolution of about 12 MeV were performed on ^{9}Be and ^{12}C. Recently, energy spectra at 700 MeV, with a resolution of 7 MeV, on seven nuclei between ^{6}Li and ^{51}V became available (HKM+72). For the light nuclei, typical $1s$ and $1p$ angular correlation distributions were observed. All these measurements are in complete agreement or are compatible with the known $(p, 2p)$ results.

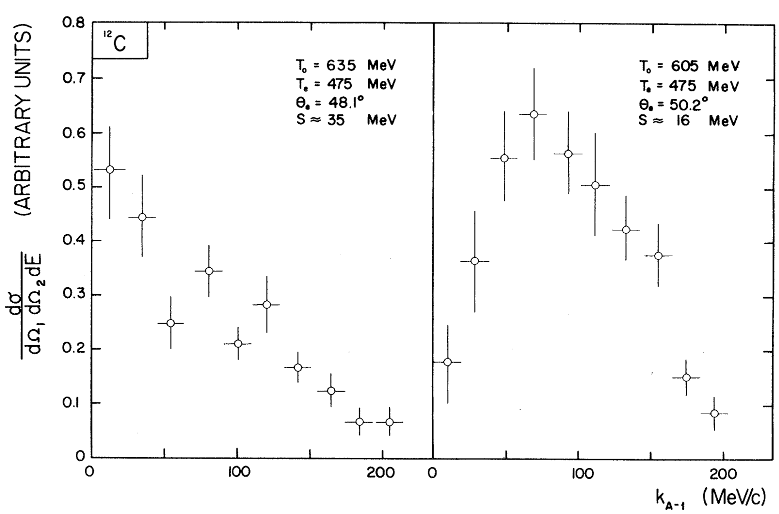

Fig. 8. Proton momentum distributions obtained from the reaction ^{12}C$(e, e'p)^{11}$B for the $1p$ and $1s$ states of ^{12}C, the incident electron energy being 605 MeV and 635 MeV, respectively; the angle of the outgoing electron was fixed, and that of the outgoing proton varied [from (ACC+67)].

In (HKM+72) distorted wave calculations were also performed, giving good agreement for ^{12}C and reasonable agreement for other nuclei. Furthermore, it has been shown with a Monte Carlo calculation that the expected multiple scattering background in ^{12}C is quite small.

The experiments performed in Saclay at 600 MeV have a resolution of 2 MeV (BMHPS71), and 1 MeV (ABD+72), respectively. Figures 9 and 10 show the results for ^{12}C and ^{40}Ca (BMHPS71). Those of ^{12}C are in agreement with earlier $(p, 2p)$ and $(e, e'p)$ experiments, but those of ^{40}Ca are at first sight somewhat surprising. The three peaks corresponding to the upper shell are clearly seen; there is some indication of the $1p$ state in the region 25–35 MeV; but there is no clear sign of the $1s$ hole state. However, taking the width of this $1s$ hole state to be about 20 MeV, which is about 10 times the experimental width of the $2s$ state, and the reduction of the peak due to distortion and to the shape of the momentum distribution to be about three times as large as that of the $2s$ state (JM62), one has a factor of about 30 in the peak height, which completely explains this result. The point is that the peaks in the energy spectrum having a small natural width increase in height with better energy resolution, whereas the height of broad peaks is practically independent of this resolution. Evidently, considerably better statistics are necessary to be able to detect the $1s$ peak in ^{40}Ca.

3.3 Summary of Experimental Results and Future Experiments

In Fig. 11 a general summary of the experimental results known at the time of writing (September 1972) is given. This graph includes the separation energies

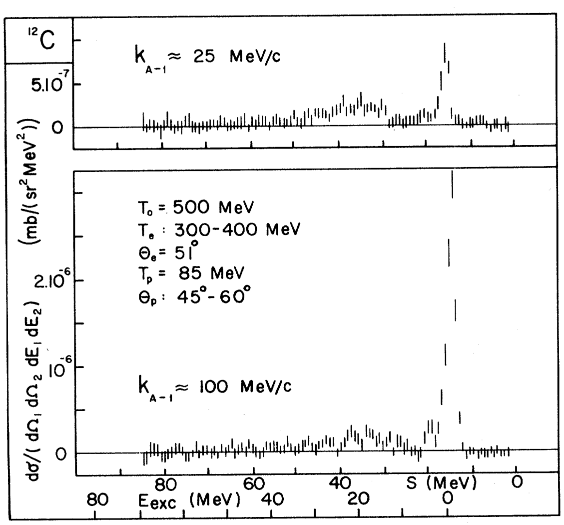

FIG. 9. Energy spectra for the reaction $^{12}C(e, e'p)^{11}B$ at two different recoil momenta obtained with energy resolution of 2 MeV; the kinematics is indicated in the figure; radiative corrections have been applied to the data [from (BMHSP71)].

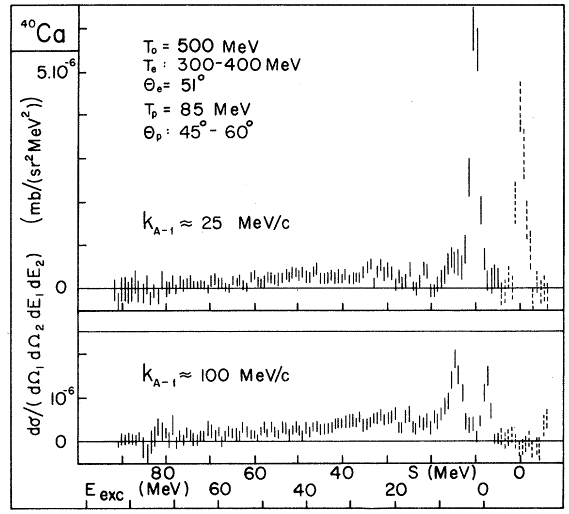

FIG. 10. Same as Fig. 9 for ^{40}Ca; the dotted bars represent contributions from hydrogen [from (BMHPS71)].

and the widths of the hole states produced in $(p, 2p)$ and $(e, e'p)$ processes and represents the only direct and detailed information available on the gross structure of inner hole states. For a comparison with results of pick-up reactions and for data on the fine structure of some $1p$ states in $2s$–$1d$ shell nuclei we refer to (BBBDR69), (Wag70), and (ABD+71). Besides the results contained in the figure, a few other scattered ones for heavier nuclei exist (ADRRR67, JAKL69); we have not included these because a more systematic investigation of the intermediate region would be necessary to follow the corresponding shells. (The references to the original experiments for the data of Fig. 11 are given in Table II.)

In the graph, the open circles and the full thin vertical lines give the energies and widths (corrected for experimental resolution where possible) of those hole states for which angular correlations have been measured and have been given a unique $l=0$ or $l\neq 0$ assignment according to the authors of the experiment or in our judgement. The interrogation signs stand for hole states where either no momentum dependence of the energy peak has been measured or where this dependence is inconclusive; dotted lines represent uncertain states. Of course the "levels" are meant in the giant resonance sense and may have a substructure. Also included in the graph (small triangles) are the separation energies of the least bound proton (MTW65) for each nucleus of interest. The heavy lines have been drawn to guide the eye through points belonging to the same shell.

At present it seems that the energy of the $1s$ hole state tends to saturate with increasing Z already for $Z=30$, at a value around 50–60 MeV, in agreement with the calculations of (Kö66). However, more experimental information is needed to confirm this statement.

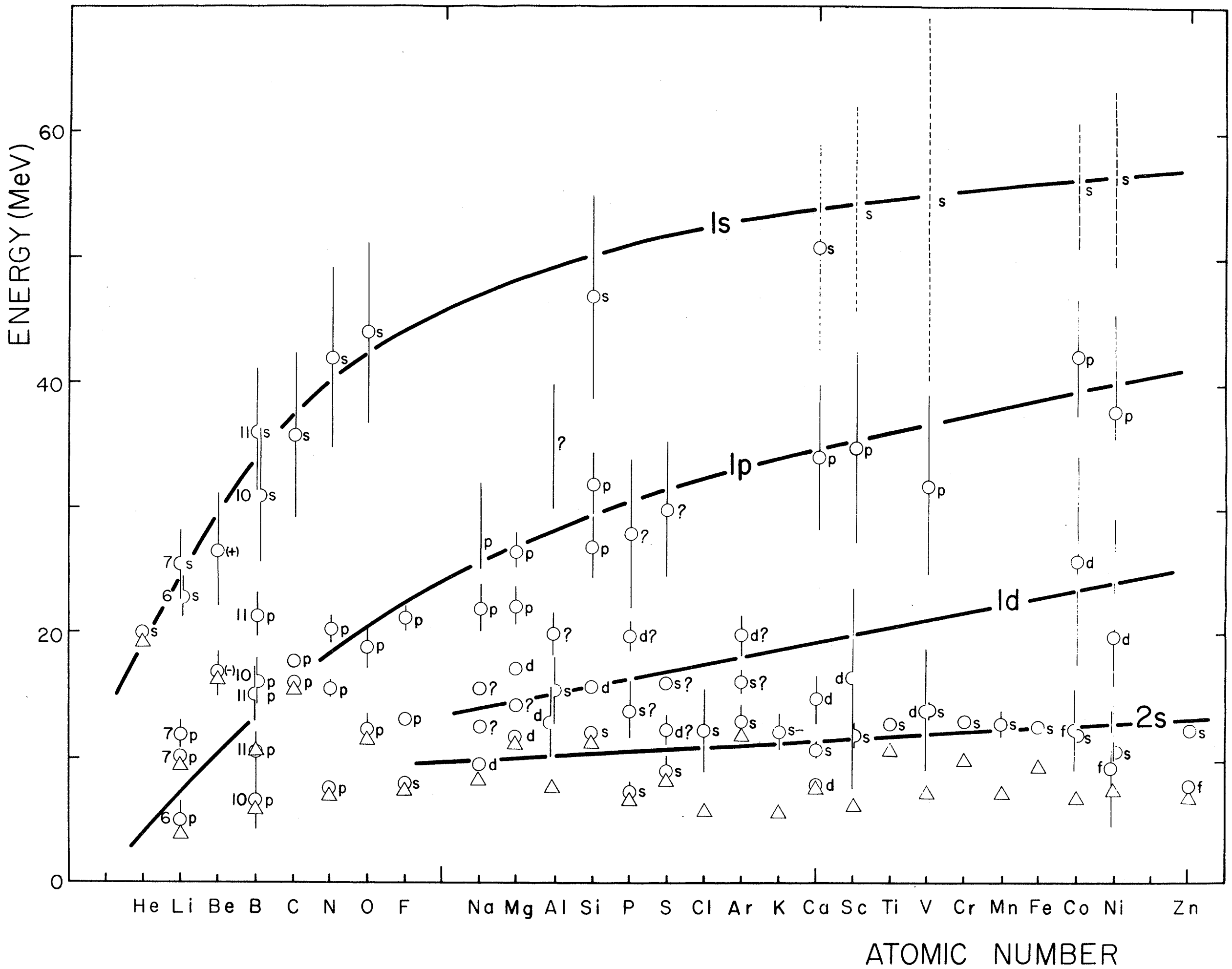

Fig. 11. Separation energies, widths (corrected for resolution where possible), and angular momentum assignments of the hole states obtained from quasi-free scattering, as functions of the atomic number (different isotopes are indicated where necessary). The angular momentum assignments are given, if reasonably unique on the basis of a measured momentum distribution, assuming the validity of the shell model. The position of a clear maximum is indicated by a circle; uncertain levels are dotted. The triangles indicate the separation energies of the least bound proton; the full lines, meant as guides for the eye, crudely follow the shells. This figure brings Fig. 11 of I up to date and includes the results given therein. The data have been obtained from the references given in Table II.

From Fig. 11 it is clear that more experiments are called for; not only $(p, 2p)$ and $(e, e'p)$ but also other types of quasi-free experiments are being presently performed or planned at several laboratories.

4. OPEN PROBLEMS

In this Section we discuss some problems which seem to be, at the best, only partially understood.

Existence of hole states: The knock-out of nucleons from strongly bound shells can result in quasi-stationary states. It is not yet established whether 1*s* hole states have been found in nuclei with $A \geq 40$, though there are indications for such states. These should be confirmed by electron experiments with sufficient resolution and statistics. The consistency of the interpretation of the observed inner shell peaks should be verified through detailed calculations, as their measured intensities are considerably larger than is expected from simple absorption arguments.

Description of hole states: Another question which immediately arises is that of how to describe most practically the hole states in strongly bound shells. One possible approximation is to start from the single-particle picture corrected with a complex rearrangement energy. The more natural one is to consider directly the wave function of a hole. In this last approximation, one could try to treat directly the hole propagator in a finite nucleus or to start from nuclear matter, construct effective hole potentials dependent on binding energy and nuclear matter density, and then make a local approximation for finite nuclei, possibly

TABLE II. References for the data presented in Fig. 11.

Nucleus	Refs.	Nucleus	Refs.	Nucleus	Refs.	Nucleus	Refs.	Nucleus	Refs.
^{4}He	a	^{12}C	a, e	^{27}Al	a	^{39}K	f	^{55}Mn	k
^{6}Li	a	^{14}N	a	^{28}Si	a, g, h	^{40}Ca	h, i, j	^{56}Fe	k
^{7}Li	a, b	^{16}O	a	^{31}P	a	^{45}Sc	j, k	^{59}Co	j, k
^{9}Be	a	^{19}F	f	^{32}S	a	^{48}Ti	k	^{58}Ni	j, k
^{10}B	a, c, d	^{23}Na	g	^{35}Cl	f	^{51}V	h, k	^{64}Zn	k
^{11}B	a, c, d	^{24}Mg	g	^{40}Ar	a	^{52}Cr	k		

[a] (TKS+66).
[b] (RAJ+67).
[c] (Ga62).
[d] (GJR+62).
[e] (GWS67).
[f] (GSW64).
[g] (ADRRR67).
[h] (LYK+71).
[i] (BMHPS71).
[j] (JAKL69).
[k] (RAD+67).

including surface corrections. Work has been started in all of these directions, but is still very incomplete.

Structure in inner shell peaks: Another question which remains to be answered is that of whether there exists a gross structure or even a fine structure in the energy peaks resulting from the knock-out of strongly bound nucleons. At present the best experiments available are the experiments in light nuclei with a resolution of about 2 MeV and not very good statistics. The expected splitting of the 1s peak in ^{6}Li, through the coupling of the total angular momenta of the p and the s shell (see I), seems in fact to have been observed (TKS+66, RAJ+67). Besides, one could also ask whether any structure in the correlation distribution for heavy nuclei is expected for large separation energies.

Short-range correlations: Short-range correlations between nucleons will in general result in highly unstable states contributing to the smooth background of the energy spectrum. Therefore, a reduction in the quasi-free cross section, due to these and other possible correlations, is expected, and for the application of sum rules to the stationary and quasi-stationary states it is important to estimate such corrections.

Structure in background: Due to their larger widths and to stronger absorption, the cross sections corresponding to inner shell states are often very small as compared to those of the more loosely bound shells. There will, of course, occur multiple collision events in which a quasi-free process in the upper shell is accompanied by an additional excitation of the residual nucleus, thus resulting in a structure in the background (see I). Such events may be located in the energy spectrum at energies where the peak resulting from quasi-free processes in inner shells is expected, but they presumably will have a smoother energy and angular dependence than these quasi-free processes. It would be interesting to estimate the magnitude and the energy and angular dependence of the correlation cross section for these "second-order" events (KLR+71), in order to avoid misinterpreting them as quasi-free processes in inner shells. This effect is, of course, much more serious for $(p, 2p)$ experiments than for $(e, e'p)$ experiments. The estimate of its size is also important for the interpretation of smaller peaks which occur and which contain a part of the strength of the single hole states.

Form factors of bound protons: Theoretically, although not experimentally, the most simple geometry for the $(e, e'p)$ experiment is one in which the parameters of the incoming and outgoing electrons are kept fixed and the momentum of the outgoing proton is varied in the plane orthogonal to the electron scattering plane. In this configuration, the main theoretical uncertainties cancel in the determination of the shape of the momentum distribution (JM62).

It was shown (De67) that the general expression for the $(e, e'p)$ cross section in the one-photon approximation is given by the distorted momentum distribution multiplied by a definite function of the proton form factors which is dependent on the experimental geometry. For the large momentum transfers under consideration, it is expected that these form factors are practically equal to the free ones, and the exact equality is in general taken for granted.

However, the nuclear binding will influence the proton form factors and it is likely, but not quite certain, that this influence is always negligible in $(e, e'p)$ experiments. It would be tempting to try to find at least an upper limit for this state dependent effect, for example in the p shell of ^{12}C or ^{16}O. This might be possible because the distorting potential varies only slightly with large changes of the energy of the outgoing proton (Sec. 2.1) and one can with good confidence correct for the resulting effect in the distorted momentum distribution (JM62, EG70). Similarly, normalization effects caused by nucleon correlations will cancel. The relevance of such an investigation for the microscopic description of nuclear structure and for the interpretation of $(e, e'p)$ experiments might justify these difficult measurements.

Variation of distortion with energy: In Sec. 2.1 it was seen that for $(p, 2p)$ processes the distorted momentum distribution is probably rather constant over a large range of incident energies and does not vary for small changes of the third parameter. This expectation should be verified both experimentally and by distorted wave calculations.

It is hoped that through the considerable experimental and theoretical efforts underway most of these problems may be solved and new ones posed.

ACKNOWLEDGMENTS

We are thankful to Miss Maria R. Teodoro and Dr. Marcus G. Zwanziger for their help in the preparation of the manuscript. We are greatly indebted to many theoretical and experimental colleagues for stimulating and helpful discussions and for communicating us their results prior to publication. Part of this work has been performed at the II. Institute for Theoretical Physics and DESY, Hamburg, Germany, and we want to thank our colleagues of these institutes for their kind hospitality. Finally, we thank the referees for useful remarks on the manuscript.

REFERENCES

ABD+71 M. Arditi, L. Bimbot, H. Doubre, N. Frascaria, J. P. Garron, M. Riou, and D. Royer, Nucl. Phys. **A165,** 129 (1971).

ABD+72 E. Auriol, A. Bussiere, J. Dupont, M. Lefevre, G. Lemarchand, J. Millaud, J. Mougey, Phan Xuan Ho, M. Priou, D. Royer, and J. Sick, Proc. Europ. Conf. Nucl. Phys. **2,** 123 (1972).

ACC+66a U. Amaldi Jr., G. Campos Venuti, G. Cortellessa, E. de Sanctis, S. Frullani, R. Lombard, and P. Salvadori, Phys. Letters **22,** 593 (1966).

ACC+66b U. Amaldi Jr., Gloria Campos Venuti, Giorgio Cortellessa, Enzo de Sanctis, Salvatore Frullani, Roselyne Lombard, and Paolo Salvadori, Acc. Naz. Lincei **41,** 494 (1966).

ACC+67 U. Amaldi Jr., G. Campos Venuti, G. Cortellessa, E. de Sanctis, S. Frullani, R. Lombard, and P. Salvadori, Phys. Letters **25B,** 24 (1967).

ADRRR67 M. Arditi, H. Doubre, M. Riou, D. Royer, and C. Ruhla, Nucl. Phys. **A103,** 319 (1967).

Am67 U. Amaldi Jr., in Proceedings of the 38th Course of the International School of Physics "Enrico Fermi" (Academic, New York, 1967), p. 284.

Am70 U. Amaldi Jr., "Elementary Processes at High Energies", in *Proceedings of the International School of Physics* (Erice, 1970, to be published.)

At68 C. Ciofi degli Atti, Nucl. Phys. **A106,** 215 (1968).

At71 C. Ciofi degli Atti, in Proc. "Adv. Inst. on Electron Scattering and Nuclear Structure", Cagliari (Gordon and Breach, New York, 1971).

Ba61 C. J. Batty, Nucl. Phys. **23,** 562 (1961).

BBAS68 S. Boffi, M. Bouten, C. Ciofi degli Atti, and J. Sawicki, Nucl. Phys. **A120,** 135 (1968).

BBBDR69 D. Bachelier, M. Bernas, I. Brissaud, C. Détraz and P. Radvanyi, Nucl. Phys. **A126,** 60 (1969).

Be65 Tore Berggren, Nucl. Phys. **72,** 337 (1965).

Be69 Tore Berggren, Proc. SIN Summerschool, Leysin (ETH, Zürich, 1969).

Be72 R. L. Becker, private communication (1972).

BJ63 Tore Berggren and Gerhard Jacob, Nucl. Phys. **47,** 481 (1963).

BKM69 V. V. Balashov, N. M. Kabachnik, and V. I. Markov, Nucl. Phys. **A129,** 369 (1969).

BMHPS71 A. Bussiere, J. Mougey, Phan Xuan Ho, M. Priou, and J. Sick, Lettere Nuovo Cimento **2,** 1149 (1971).

BMP72 K. A. Brueckner, H. W. Meldner, and J. D. Perez, Phys. Rev. C **6,** 773 (1972).

BP70 Richard L. Becker and M. R. Patterson, Bull. Am. Phys. Soc. **15,** 1315 (1970).

BPS68 S. Boffi, F. D. Pacati, and J. Sawicki, Nuovo Cimento **57B,** 103 (1968).

BT66 Tore Berggren and Helge Tyrén, Ann. Rev. Nucl. Sci. **16,** 153 (1966).

CCC+72 G. Campos Venuti, G. P. Capitani, G. Cortellessa, E. de Sanctis, G. Farchi, S. Frullani, R. Giordano, P. Salvadori, and K. Takamatsu, "Distribuzioni Angolari dei Protoni nel Calcio con la Reazione $(e, e'p)$," Preprint ISS72/9 (1972).

Co76 G. Cortellessa, Suppl. Nuovo Cimento **3,** 820 (1965).

CS66 Gloria Campos Venuti and Paolo Salvadori, Ann. Ist. Super. Sanità **2,** 764 (1966).

CT69 I. E. McCarthy and A. W. Thomas, Nucl. Phys. **A135,** 463 (1969).

De67 V. Devanathan, Ann. Phys. (N.Y.) **43,** 74 (1967).

DS63 J. Dabrowski and A. Sobiczewski, Phys. Letters **5,** 87 (1963).

EG70 C. D. Epp and T. A. Griffy, Phys. Rev. **C1,** 1633 (1970).

EW72 C. A. Engelbrecht and H. A. Weidenmüller, Nucl. Phys. **A184,** 385 (1972).

Fa71 B. Favier, "Section Efficace Totale $p-{}^{12}C$ Entre 190 et 560 MeV," Preprint CERN/MSC 71-4 (1971)

Fo67 Taber de Forest Jr., Ann. Phys. (N.Y.) **45,** 365 (1967).

FW53 N. C. Francis and K. M. Watson, Phys. Rev. **92,** 291 (1953).

FW71 Alexander L. Fetter and John Dirk Walecka, *Quantum Theory of Many-Particle Systems* (McGraw–Hill, New York, 1971).

Ga62 Jean-Pierre Garron, Ann. Phys. (Paris) **7,** 301 (1962).

GB60 A. M. Green and G. E. Brown, Nucl. Phys. **18,** 1 (1960).

GB71 Christer Gustafsson and Tore Berggren, Phys. Letters **35B,** 546 (1971).

GJR+62 J. P. Garron, J. C. Jacmart, M. Riou, C. Ruhla, J. Teillac, and K. Strauch, Nucl. Phys. **37,** 126 (1962).

GL70 D. H. E. Gross and R. Lipperheide, Nucl. Phys. **A150,** 449 (1970).

Go48 M. L. Goldberger, Phys. Rev. **74,** 1269 (1948).

GSW64 B. Gottschalk, K. Strauch, and K. H. Wang, Compt. Rend. Congr. Intern. Phys. Nucl. Vol. 2 (C.N.R.S., Paris, 1964) p. 324, and private communication from K. Strauch.

GWS67 B. Gottschalk, K. H. Wang, and K. Strauch, Nucl. Phys. **A90,** 83 (1967) referred to as Harvard experiment.

He71 Victoria E. Herscovitz, Nucl. Phys. **A161,** 321 (1971).

HFG71 T. A. Hughes, S. Fallieros, and B. Goulard, Particles and Nuclei **2,** 93 (1971).

HJM68 Victoria E. Herscovitz, Gerhard Jacob, and Th. A. J. Maris, Nucl. Phys. **A109,** 478 (1968).

HJMS71 V. E. Herscovitz, G. Jacob, Th. A. J. Maris, and C. Schneider, Rev. Bras. Fis. **1,** 43 (1971).

HKM+70 S. Hiramatsu, T. Kamae, H. Muramatsu, K. Nakamura, K. Nishiyama, Y. Shimizu, and S. Kabe, "Quasi free Electron Scattering on ^{12}C and ^{9}Be," Preprint INS J–122 (1970).

HKM+72 S. Hiramatsu, T. Kamae, H. Muramatsu, K. Nakamura, N. Izutsu, and Y. Watase, "$(e, e'p)$ Reaction on ^{6,7}Li, ^{9}Be, ^{12}C, ^{27}Al, ^{40}Ca and ^{51}V; Quasi-free Electron Scattering on Light Nuclei," Preprint (1972).

Jac68 Daphne F. Jackson, Adv. Phys. **17,** 481 (1968).

Jai68 B. K. Jain, Nucl. Phys. **A116,** 256 (1968).

Ja71 Daphne F. Jackson, Adv. Nucl. Phys. **4,** 1 (1971).

JABCL69 A. N. James, P. T. Andrews, P. Butler, N. Cohen, and B. G. Lowe, Nucl. Phys. **A133,** 89 (1969), referred to as Liverpool experiment.

JAKL69 A. N. James, P. T. Andrews, P. Kirkby, and B. G. Lowe, Nucl. Phys. **A138,** 145 (1969), referred to as Liverpool experiment.

JJ67 B. K. Jain and Daphne F. Jackson, Nucl. Phys. **A99,** 113 (1967).

JM60 Gerhard Jacob and Th. A. J. Maris, Nucl. Phys. **20,** 440 (1960).

JM62 Gerhard Jacob and Th. A. J. Maris, Nucl. Phys. **31,** 139 and 152 (1962).

JM66 Gerhard Jacob and Th. A. J. Maris, Rev. Mod. Phys. **38,** 121 (1966), referred to as I.

KLR+71 S. Kullander, F. Lemeilleur, P. U. Renderg, G. Landaud, J. Yonnet, B. Fagerström, A. Johansson, and G. Tibell, Nucl. Phys. **A173,** 357 (1971), referred to as CERN experiment.

KMT59 A. K. Kerman, H. McManus, and R. M. Thaler, Ann. Phys. (N.Y.) **8,** 551 (1959).

Kö66 H. S. Köhler, Nucl. Phys. **88,** 529 (1966).

Ko72 Daniel S. Koltun, Phys. Rev. Lett. **28,** 182 (1972).

KRF+71 S. Kullander, P. U. Renberg, B. Fagerström, A. Johansson, G. Tibell, G. Landaud, F. Lemeilleur, and J. Yonnet, Phys. Letters **34B,** 197 (1971), referred to as CERN experiment.

KS67 Yoshiteru Kudo and Shota Suekane, Progr. Theoret. Phys. (Kyoto) **38,** 520 (1967).

KS69 V. M. Kolybasov and N. Ya. Smorodinskaya, Nucl. Phys. **A136,** 165 (1969).

Ku69 S. Kullander, Prog. SIN Summerschool, Leysin (ETH, Zürich, 1969).

LMT59 R. H. Lemmer, Th. A. J. Maris and Y. C. Tang, Nucl. Phys. **12,** 619 (1959).

LYK+71 G. Landaud, J. Yonnet, S. Kullander, F. Lemeilleur, P. U. Renberg, B. Fagerström, A. Johansson, and G. Tibell, Nucl. Phys. **A173,** 337 (1971), referred to as CERN experiment.

Ma58/59 Th. A. J. Maris, Nucl. Phys. **9,** 577 (1958/59).

MHT58 Th. A. J. Maris, Peter Hillman, and H. Tyrén, Nucl. Phys. **7,** 1 (1958).

MP71 H. W. Meldner and J. D. Perez, Phys. Rev. A **4,** 1388 (1971).

MTW65 J. H. E. Mattauch, W. Thiele, and A. H. Wapstra, Nucl. Phys. **67,** 1 (1965).

PA72 S. Pittel and N. Austern, Phys. Rev. Letters **29,** 1403 (1972).

PB72 Lucy W. Person and Paul Benioff, Nucl. Phys. **A187,** 401 (1972).

PSG+69 C. F. Perdrisat, L. W. Swenson, P. C. Gugelot, E. T. Boschitz, W. K. Roberts, J. S. Vincent, and J. R. Priest, Phys. Rev. **187,** 1201 (1969).

Ra72a S. Radhakant, Nucl. Phys. **A188,** 353 (1972).

Ra72b S. Radhakant, Phys. Lett. **40B,** 70 (1972).

RAD+67 C. Ruhla, M. Arditi, H. Doubre, J. C. Jacmart, M. Liu, R. A. Ricci, M. Riou, and J. C. Roynette, Nucl. Phys. **A95,** 526 (1967).

RAJ+67 J. C. Roynette, M. Arditi, J. C. Jacmart, F. Mazloum, M. Riou, and C. Ruhla, Nucl. Phys. **A95,** 545 (1967).

RR69 M. Riou and Ch. Ruhla, Progr. Nucl. Phys. **2,** 195 (1969).

RSL70 Edward F. Redish, G. J. Stephenson, Jr. and Gerald M. Lerner, Phys. Rev. **C2,** 1665 (1970).

SFP+70 W. D. Simpson, J. L. Friedes, H. Palevsky, R. J. Sutter, G. W. Bennett, B. Gottschalk, G. Igo, R. L. Stearns, N. S. Wall, D. M. Corley, and G. C. Phillips, Nucl. Phys. **A140,** 201 (1970), referred to as Brookhaven experiment.

SJ71 R. Shanta and B. K. Jain, Nucl. Phys. **175,** 417 (1971).

SRLH72 G. J. Stephenson Jr., Edward F. Redish, Gerald M. Lerner, and M. I. Haftel, "$(p, 2p)$ Reactions with Divers Potentials," Maryland Technical Report No. 73–002 (1972).

THM58 H. Tyrén, Peter Hillman, and Th. A. J. Maris, Nucl. Phys. **7,** 10 (1958).

TKS+66 H. Tyrén, S. Kullander, O. Sundberg, R. Ramachandran, P. Isacsson, and T. Berggren, Nucl. Phys. **79,** 321 (1966), and private communication from H. Tyrén.

TMH57 H. Tyrén, Th. A. J. Maris, and P. Hillman, Nuovo Cimento **6,** 1507 (1957).

Üb71 Herbert Überall, *Electron Scattering from Complex Nuclei B* (Academic, New York, 1971).

VA71 Raoul D. Viollier and Kurt Alder, Helv. Phys. Acta **44,** 77 (1971).

Wa53 Kenneth M. Watson, Phys. Rev. **89,** 575 (1953).

Wa68 A. Watt, Phys. Lett. **27B,** 190 (1968).

Wag70 Gerhard J. Wagner, Habilitationsschrift, MPI H–V8 (1970), unpublished.

WC66 Karl Wildermuth and Walter McClure, in Springer Tracts in Mod. Phys. (Springer Verlag, Berlin, 1966), Vol. 41, p. 1.

WGL71 U. Wille, D. H. E. Gross, and R. Lipperheide, Phys. Rev. C **4,** 1070 (1971).

Wi68 Denys H. Wilkinson, Comm. Nucl. and Part. Phys. **2,** 48 (1968).

Wi71 Uwe Wille, Ph.D. Thesis, Freie Universität Berlin (1971) unpublished.

WL72 U. Wille and R. Lipperheide, Nucl. Phys. **A189,** 113 (1972).

YH67 T. Yuasa and E. Hourany, Nucl. Phys. **A103,** 577 (1967).